ACS SENSORS

pubs.acs.org/acssensors

Letter

Graphene Field Effect Transistor-Based Immunosensor for Ultrasensitive Noncompetitive Detection of Small Antigens

Yasushi Kanai,[▽] Yuki Ohmuro-Matsuyama,[▽] Masami Tanioku, Shota Ushiba, Takao Ono, Koichi Inoue, Tetsuya Kitaguchi, Masahiko Kimura, Hiroshi Ueda,[*] and Kazuhiko Matsumoto

Cite This: *ACS Sens.* 2020, 5, 24−28

Read Online

ACCESS | Metrics & More | Article Recommendations | Supporting Information

ABSTRACT: Due to its high carrier mobility, graphene is considered a suitable material for use in field-effect transistors. However, its application to immunosensing of small molecules is still elusive. To investigate the potential of graphene field effect transistors (G-FET) as a sensor for small molecules with small or no charge, we applied the open-sandwich immunoassay (OS-IA), which detects low-molecular-weight antigens noncompetitively, to G-FET. Using an antibody variable fragment V_L immobilized on graphene and a hyperacidic region of amyloid precursor protein fused to the other variable fragment V_H, we successfully detected a small antigen peptide consisting of 7 amino acids (BGP-C7), with a more than 100-fold increase in sensitivity compared with that measured by enzyme-linked OS-IA. Furthermore, we succeeded in detecting BGP-C7 in the presence of human serum with similar sensitivity, suggesting its potential application in clinical diagnostics.

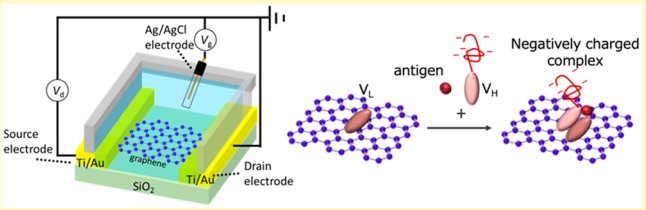

KEYWORDS: *electrochemical biosensor, immunosensor, clinical diagnostics, graphene, amyloid precursor protein, antibody variable region, fusion protein*

Immunoassays are used to detect and quantify specific targets in various fields, such as basic biology,[1] clinical diagnostics,[2−5] food sanitation management,[6−8] and environmental preservation.[9−11] Establishment of a sensitive and quick method of antigen detection is desirable for immunoassays. We previously developed an open-sandwich immunoassay (OS-IA), in which the two antibody variable region fragments, V_H and V_L, were isolated from an antibody using recombinant DNA technology.[12,13] The underlying principle is that V_H and V_L have low affinity for one another in the absence of an antigen; however, when the antigen is added, the affinity dramatically increases, and a V_H-antigen-V_L complex is formed (Figure 1A).[14] This is due to the bridging of two V region fragments by the bound antigen (ca., ligand), which leads to higher stability of the resulting complex, especially when the size of antigen is small enough to be captured inside the cavity formed by the two fragments. The principal advantage of the OS-IA is that many antigens of low molecular weight, such as a bone disease marker,[15] an endocrine disruptor,[16] an aromatic aldehyde,[17] thyroxine,[18] specific protein phosphorylation,[19] and oxidized lipids[20] can be detected with higher sensitivity and a wider detection range than that when using corresponding competitive IAs.[14]

The enzyme linked immunosorbent assay (ELISA) is the most popularly used assay format for OS-IAs. In OS-ELISA, the V_L (or V_H) is immobilized on the surface of the wells in an assay plate, after which the V_H (or V_L) is added along with the sample. Depending on the antigen concentration, the V_H (or V_L) binds to the immobilized V_L (or V_H) (Figure 1B). Next, the wells are washed, and the V_H (or V_L) that remains attached

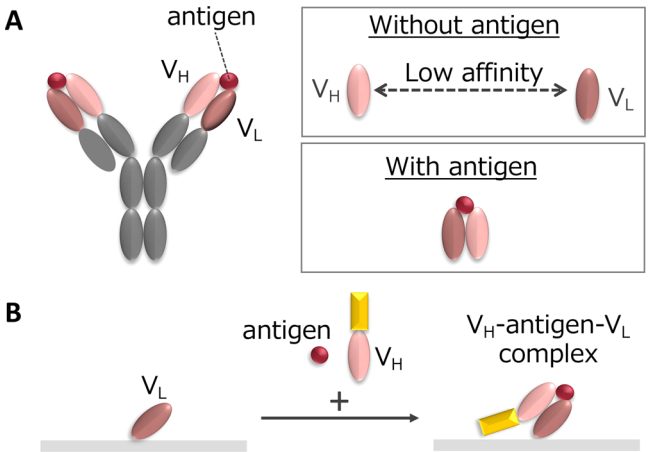

Figure 1. OS-IA: (A) Principle of OS-IA. (B) Scheme of OS-IA. In the case of OS-ELISA, enzyme is attached to V_H as a label (marked yellow).

Received: October 31, 2019
Accepted: January 10, 2020
Published: January 10, 2020

https://dx.doi.org/10.1021/acssensors.9b02137
ACS Sens. 2020, 5, 24−28

is detected by the use of a labeled enzyme, which shows an antigen-dependent signal. Due to its noncompetitive detection mode and the wide availability of suitable antibodies that recognize small antigens (haptens), many small molecules such as medicines comprising steroids or peptides or chemical substances and toxins that contaminate food, water, and the environment have been successfully measured to date.[14]

In this study, we applied an OS-IA to a graphene field effect transistor (G-FET) and attempted to make an immunosensor for an antigen peptide comprising only 7 amino acids. Semiconductor FET biosensors are portable devices that can integrate several laboratory functions on a chip. In these FETs, G-FET is suitable as a highly sensitive biosensor because of the high electron mobility and chemical stability of graphene.[21−27] A change in the electrical conductivity of graphene in the G-FET leads to a change in the electric current between the source and the drain ΔI_d (Figure 2A). Therefore, when targets

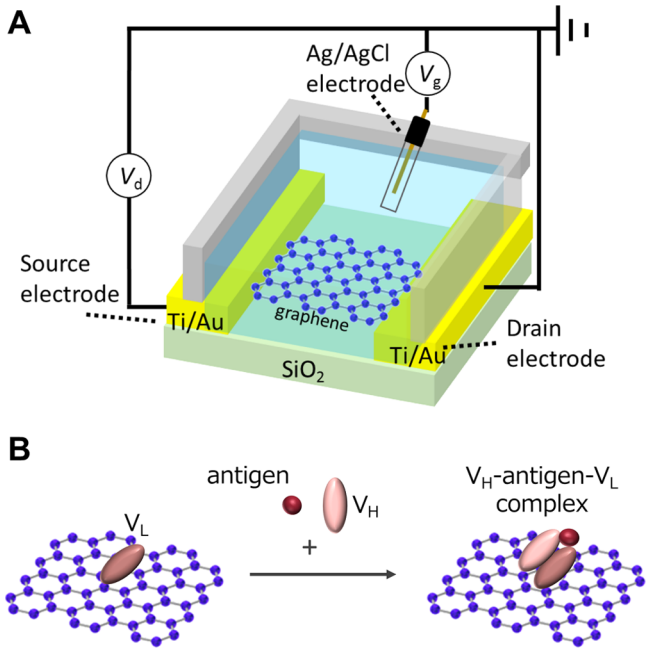

Figure 2. Graphene field effect transistor (G-FET) and its application to OS-IA: (A) Schematic structure of G-FET. (B) Scheme of OS-IA using G-FET. The V_H fragment can be tethered with a charged protein to attain an enhanced signal.

bind to the surface of graphene, the electrical conductivity of graphene changes due to the charge of the targets, and targets can be detected. Although we previously used silicon FETs for the OS-IA,[16] graphene, unlike other semiconductors such as silicon-based ones,[16,28−31] can be directly modified without oxidation layers; further, the electron mobility of graphene is higher than that of silicon. Therefore, it is expected that G-FETs will be more sensitive to the charge of the target. Here, we used the G-FET to perform an OS-IA for the detection of small molecules. Although the sensitivity of the G-FET is high, the detection of small molecules has been a challenge because of their small charge and Debye length. One potential advantage of performing an OS-IA with an FET instead of performing the conventional competitive immunoassay for small molecules is that the former uses only the variable region fragments (~12 kDa), which are much smaller than the entire antibody (~150 kDa). In the assay, the V_L fragment derived from an antibody is immobilized on graphene, and then the V_H fragment from the same antibody is added along with a sample containing variable amounts of antigen. The current change in graphene due to the binding of V_H is expected to be higher than that of antigen alone, because of the higher charge of V_H itself or of the tagged charged protein bound (Figure 2B).

In this study, the recombinant variable region fragments of the anti-bone Gla protein (BGP or osteocalcin) antibody were prepared and used for OS-IAs to detect BGP-C7, a C-terminal 7-mer peptide of human osteocalcin (bone gla protein, BGP), which is a minor bone protein utilized as a bone disease marker. Recently, BGP has also attracted attention for its unprecedent functions in glucose homeostasis,[32] brain development,[33] and male fertility.[34] First, the antigen-dependent interaction between the prepared thioredoxin (Trx), biotin acceptor peptide (BAP)-fused V_H, and maltose binding protein (MBP)-fused V_L was confirmed using OS-ELISA (Figure S1A).

To perform OS-IA using a G-FET, the graphene part of the FET, which was synthesized on copper foils by a chemical vapor deposition method, was coated with 1-pyrenebutanoic acid succinimidyl ester (PBASE), and MBP-V_L was reacted with PBASE to immobilize it with short distance. The transconductance of the G-FET g_m was evaluated based on the transport characteristics in 10 mM phosphate buffer (PB, pH 7.0) and 1 μg/mL Trx-BAP-V_H solution (Figure S2). A constant concentration of Trx-BAP-V_H and varying concentrations of BGP-C7 were added to graphene, and the value of the normalized drain current change ($\Delta I_d/g_m$) was measured (Figures S2 and S3) at source drain voltage V_d = −0.1 V and gate voltage V_g = 0.1 V. An increasing concentration of BGP-C7 was added at equal time intervals, and the final concentration was adjusted to 10^{-1}, 1, 10^1, 10^2, and 10^3 ng/mL. We found that the value of $\Delta I_d/g_m$ (V) did not significantly increase with the increase in the concentration of BGP-C7.

We reasoned that the negative charge of added Trx-BAP-V_H was not large enough to allow for the sensitive amplification of the drain current. Next, to enhance the current change of the G-FET by the binding of V_H, V_H was fused to an APP tag derived of an intrinsically disordered region[35] of murine amyloid precursor protein[36] that contains many acidic amino acids, i.e., aspartic acid (D) and glutamic acid (E), to attain a higher negative charge (Figure 3A). In 10 mM phosphate buffer, the Debye layer thickness (Debye length) is about 3 nm. The size of V_H-antigen-V_L complex is also the same (~3 nm diameter). From the N-terminus of V_H, the flexible and negatively charged APP moiety will move around and is expected to come closer to graphene surface. The addition of APP tag was also favorable to enhance the solubility of fusion protein, which increased its expression in *E. coli* cytoplasm. It was confirmed by antigen-binding ELISA that the APP tag-fused V_H was functional and could bind to V_L and BGP-C7 (Figure S1B). The MBP-fused V_L fragment was immobilized on the graphene via PBASE as before. Figure 3B shows the $\Delta I_d/g_m$ value at several concentrations of BGP-C7, V_d = −0.1 V and V_g = 0 V. The hole current ($\Delta I_d/g_m$) increased depending on the concentration of BGP-C7 up to 100 ng/mL, which indicates that negative ions were adsorbed on graphene surfaces. Because BGP-C7 and V_H bind V_L on graphene surfaces, $\Delta I_d/g_m$ was changed by negative ions in the disordered APP tag-fused on V_H. Compared to the results seen in Figures 3B and S3, the APP tag fused on V_H made the

https://dx.doi.org/10.1021/acssensors.9b02137
ACS Sens. 2020, 5, 24−28

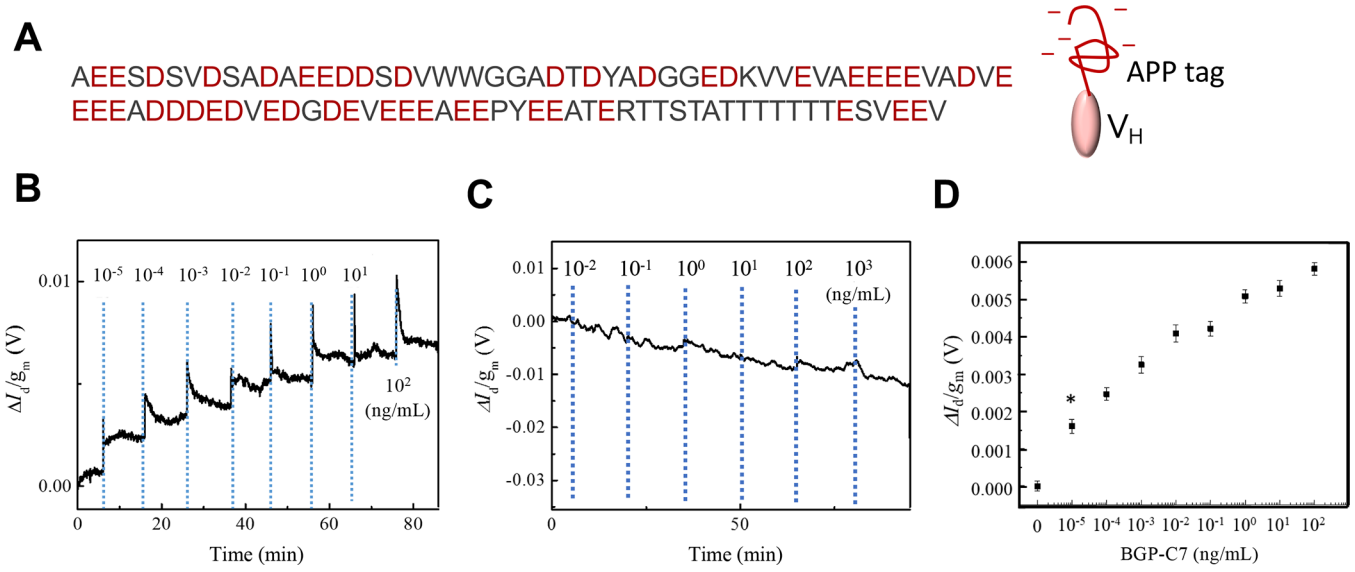

Figure 3. Use of APP-V_H as a hyper acidic detector. (A) Amino acid sequence of APP tag. (B,C) Time course of average $\Delta I_d/g_m$ at V_d of 0.1 V, V_g of 0 V for V_L modified G-FETs, various concentrations of BGP-C7 (B) and BGP-C10dV (C) and a constant concentration of APP-V_H of 1 μg/mL. (D) Dose-dependency plot. Error bar, ±1 SD. *LOD.

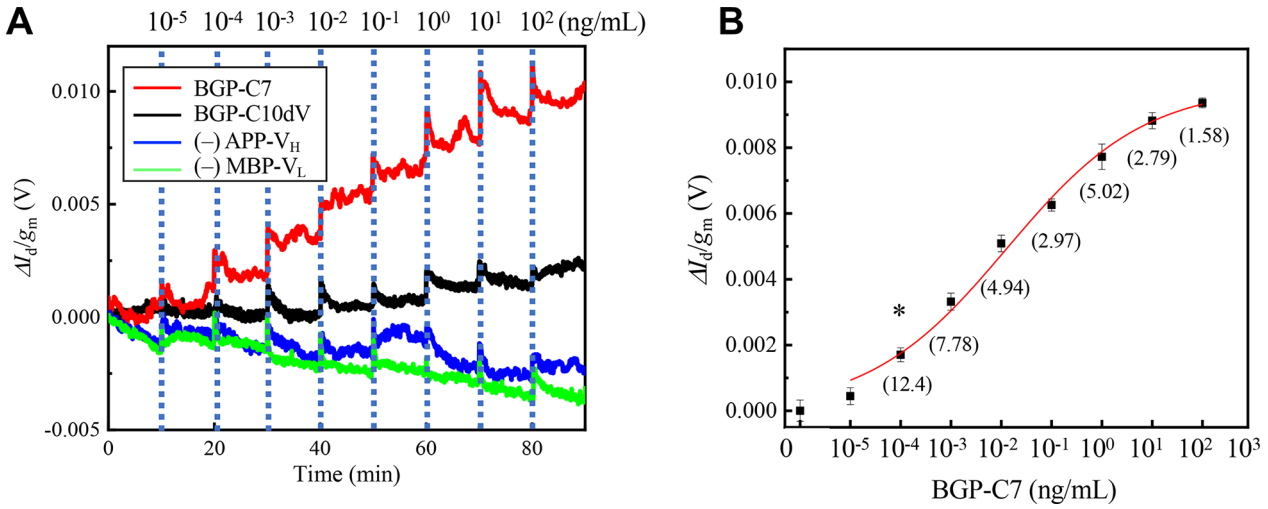

Figure 4. Measurement in 0.5% human serum. (A) Time course of average $\Delta I_d/g_m$ at V_d of 0.1 V, V_g of 0 V for V_L modified G-FETs, various concentrations of BGP-C7 (red) or BGP-C10dV (black) with constant concentration of APP-V_H of 1 μg/mL were applied. As a control, BGP-C7 alone (blue) was applied to V_L modified G-FET, whereas BGP-C7 and APP-V_H were applied to intact G-FET without V_L (green). (B) Dose-dependency plot. Error bars represent ±1 SD. RSD (%) of each point is shown in the parentheses. *LOD.

G-FETs more sensitive to detect BGP-C7. Figure 3C shows the $\Delta I_d/g_m$ value at several concentrations of BGP-C10dV; BGP-C10dV has a sequence very similar to that of BGP-C7 but does not bind to this antibody that specifically recognizes the C-terminal valine residue of BGP. $\Delta I_d/g_m$ did not increase by addition of BGP-C10dV, which indicates that G-FETs do not detect BGP-C10dV. These results indicate that G-FETs can detect BGP-C7 selectively. The limit of detection (LOD) of BGP-C7 was dramatically improved to 10 fg/mL (Figures S3, Figure 3B). The sensitivity in terms of the LOD was more than 100-fold higher than that of OS-ELISA using this antibody.

Furthermore, to investigate the possible use of this system in clinical diagnostics, the samples were measured in the presence of 0.5% human serum in PB (Figures S3, C and D, and Figure 4A). We found that the current increased depending on the concentration of BGP-C7 up to 1000 ng/mL, although the current increase on addition of BGP-C10dV was very small. Taken together, G-FETs can detect BGP-C7 selectively, and have a low LOD (100 fg/mL) for BGP-C7 in 0.5% serum (Figure 4B). This concentration translates to 20 pg/mL of BGP-C7 (mw: 894) in 100% serum. Since the normal ranges of osteocalcin (mw: ~6 k) in Japan for healthy women are 7.8−30.8 ng/mL and 14.2−54.8 ng/mL before and after menopause, respectively, and 8.4−33.1 ng/mL for men, the obtained LOD (~130 pg/mL) and the working range are sufficient enough to cover all these ranges.

There could be four possible reasons for the considerable improvement of the sensitivity and detection range. First, G-FETs are suitable for use in immunoassays because of the high electron mobility of graphene, which causes a large current change by binding the probe. The second reason is the application of the OS-IA, which can be used for the detection of small molecules with high sensitivity. Although small

https://dx.doi.org/10.1021/acssensors.9b02137
ACS Sens. 2020, 5, 24−28

antigens typically have small electric charges, one of the probes (APP-V_H), which has a larger negative charge than the charge of the small antigen, binds to graphene with the antigen leading current change by not only the charge of the antigen but also the charge of one of the bound probes. The third reason is the fusion of V_H to the flexible APP tag containing many acidic amino acids. This fusion dramatically increased the negative charge of the probe bound to graphene and led to a large change in the current detected by the FET. Probably, the intrinsically unstructured and hyperacidic nature of APP has enabled its spatial approximation to the graphene surface. The fourth reason is the effect of the electrical potential near the graphene surface. We applied a negative voltage on graphene (V_d) and a positive voltage on the solution due to the standard potential of Ag/AgCl (~0.2 V). Hence, the positive ions in the solution move to the graphene surface. The concentration $n(\phi)$ is described by the Boltzmann distribution

$$n(\phi) = n(0)\exp(-q\phi/k_BT)$$

where ϕ is the potential, $n(0)$ is the concentration in the solution at 0 V, q is the charge amount of the ion, k_B is the Boltzmann's constant, and T is the temperature. As two positive ions exist in BGP-C7 and the ϕ is 0 ~ −0.3 V near the graphene surface, the concentration of BGP-C7 could be condensed about 10^{10} times at a maximum on the graphene surface.

We applied the OS-IA to the G-FET for the detection of a small antigen with high sensitivity. The use of the G-FETs resulted in a 100-fold higher sensitivity, mainly due to the use of APP tag-fused V_H and the wider antigen detection range than that of OS-ELISA was attained. To date, although many graphene- or carbon nanotube-based immunosensors[37] and other affinity sensors[38] are reported, very few report detection of small molecules.[39−41] The high sensitivity attained with our sensor even in the presence of human serum suggests its potential application in clinical diagnostics.

■ ASSOCIATED CONTENT

Supporting Information

The Supporting Information is available free of charge at https://pubs.acs.org/doi/10.1021/acssensors.9b02137.

SI Materials and Methods (PDF)

■ AUTHOR INFORMATION

Corresponding Author

Hiroshi Ueda − *Tokyo Institute of Technology, Yokohama, Japan;* orcid.org/0000-0001-8849-4217; Email: ueda@res.titech.ac.jp

Other Authors

Yasushi Kanai − *Osaka University, Ibaraki, Japan*

Yuki Ohmuro-Matsuyama − *Tokyo Institute of Technology, Yokohama, Japan*

Masami Tanioku − *Osaka University, Ibaraki, Japan*

Shota Ushiba − *Murata Manufacturing Co. Ltd., Nagaokakyo-shi, Japan;* orcid.org/0000-0001-7652-081X

Takao Ono − *Osaka University, Ibaraki, Japan;* orcid.org/0000-0002-6717-123X

Koichi Inoue − *Osaka University, Ibaraki, Japan*

Tetsuya Kitaguchi − *Tokyo Institute of Technology, Yokohama, Japan;* orcid.org/0000-0001-6701-1933

Masahiko Kimura − *Murata Manufacturing Co. Ltd., Nagaokakyo-shi, Japan*

Kazuhiko Matsumoto − *Osaka University, Ibaraki, Japan*

Complete contact information is available at: https://pubs.acs.org/10.1021/acssensors.9b02137

Author Contributions

[∇]The manuscript was written through the contribution of all authors. All authors have approved the final version of the manuscript. Y.K. and Y.O.-M. contributed equally.

Funding

This work was supported in part by JSPS KAKENHI Grant Numbers JP18H03851 (to H.U.), JP17K06920 (to Y.O.M.), and JP19H02582 (to Y.K.) from the Japan Society for the Promotion of Science, Japan, and by JST-Mirai Grant Number JPMJMI18D9 (to H.U.) and JST-CREST Grant Number JPMJCR15F4 (to K.M.) from Japan Science and Technology Agency, Japan.

Notes

The authors declare no competing financial interest.

■ ACKNOWLEDGMENTS

We thank the Biomaterials Analysis Division, Technical Department, Tokyo Institute of Technology for DNA sequence analysis, and the support by Dynamic Alliance for Open Innovation Bridging Human, Environment and Materials from MEXT, Japan.

■ REFERENCES

(1) DeLaney, K.; Buchberger, A. R.; Atkinson, L.; Grunder, S.; Mousley, A.; Li, L. New techniques, applications and perspectives in neuropeptide research. *J. Exp. Biol.* **2018**, *221*, jeb151167.

(2) Balahura, L. R.; Stefan-Van Staden, R. I.; Van Staden, J. F.; Aboul-Enein, H. Y. Advances in immunosensors for clinical applications. *J. Immunoassay Immunochem.* **2019**, *40* (1), 40−51.

(3) Engin, E. D. The use of multiplexing technology in the immunodiagnosis of infectious agents. *J. Immunoassay Immunochem.* **2019**, *40* (1), 109−122.

(4) Horber, S.; Achenbach, P.; Schleicher, E.; Peter, A. Harmonization of immunoassays for biomarkers in diabetes mellitus. *Biotechnol. Adv.* **2019**, DOI: 10.1016/j.biotechadv.2019.02.015.

(5) Saraswati, K.; Phanichkrivalkosil, M.; Day, N. P. J.; Blacksell, S. D. The validity of diagnostic cut-offs for commercial and in-house scrub typhus IgM and IgG ELISAs: A review of the evidence. *PLoS Neglected Trop. Dis.* **2019**, *13* (2), No. e0007158.

(6) Chen, W.; Huang, Z.; Hu, S.; Peng, J.; Liu, D.; Xiong, Y.; Xu, H.; Wei, H.; Lai, W. Invited review: Advancements in lateral flow immunoassays for screening hazardous substances in milk and milk powder. *J. Dairy Sci.* **2019**, *102* (3), 1887−1900.

(7) Do, A. B.; Khuda, S. E.; Sharma, G. M. Undeclared Food Allergens and Gluten in Commercial Food Products Analyzed by ELISA. *J. AOAC Int.* **2018**, *101* (1), 23−35.

(8) Rahman, H. U.; Yue, X.; Yu, Q.; Xie, H.; Zhang, W.; Zhang, Q.; Li, P. Specific Antigen Based and Emerging Detection Technologies of Mycotoxins. *J. Sci. Food Agric.* **2019**, *99* (11), 4869−4877.

(9) Fang, T. Y.; Praveena, S. M.; deBurbure, C.; Aris, A. Z.; Ismail, S. N. S.; Rasdi, I. Analytical techniques for steroid estrogens in water samples - A review. *Chemosphere* **2016**, *165*, 358−368.

(10) Behera, B. K.; Das, A.; Sarkar, D. J.; Weerathunge, P.; Parida, P. K.; Das, B. K.; Thavamani, P.; Ramanathan, R.; Bansal, V. Polycyclic Aromatic Hydrocarbons (PAHs) in inland aquatic ecosystems: Perils

and remedies through biosensors and bioremediation. *Environ. Pollut.* **2018**, *241*, 212−233.
(11) Daniels, T.; Earlywine, M.; Breeding, V. Environmental services impact on healthcare-associated Clostridium difficile reduction. *Am. J. Infect. Control* **2019**, *47* (4), 400−405 e1.
(12) Ueda, H.; Tsumoto, K.; Kubota, K.; Suzuki, E.; Nagamune, T.; Nishimura, H.; Schueler, P. A.; Winter, G.; Kumagai, I.; Mahoney, W. C. Open sandwich ELISA: A novel immunoassay based on the interchain interaction of antibody variable region. *Nat. Biotechnol.* **1996**, *14* (13), 1714−1718.
(13) Ueda, H. Open sandwich immunoassay: a novel immunoassay approach based on the interchain interaction of an antibody variable region. *J. Biosci. Bioeng.* **2002**, *94* (6), 614−619.
(14) Dong, J.; Ueda, H. Open sandwich immunoassay and its applications. In *Advances in Medicine and Biology*, Berhardt, L. V., Ed.; Nova Science Publishers Inc.: New York, 2017; Vol. *125*, pp 123−159.
(15) Lim, S. L.; Ichinose, H.; Shinoda, T.; Ueda, H. Noncompetitive detection of low molecular weight peptides by open sandwich immunoassay. *Anal. Chem.* **2007**, *79* (16), 6193−6200.
(16) Sakata, T.; Ihara, M.; Makino, I.; Miyahara, Y.; Ueda, H. Open Sandwich-Based Immuno-Transistor for Label-Free and Noncompetitive Detection of Low Molecular Weight Antigen. *Anal. Chem.* **2009**, *81* (18), 7532−7537.
(17) Shirasu, N.; Onodera, T.; Nagatomo, K.; Shimohigashi, Y.; Toko, K.; Matsumoto, K. Noncompetitive immunodetection of benzaldehyde by open sandwich ELISA. *Anal. Sci.* **2009**, *25*, 1095−1100.
(18) Islam, K. N.; Ihara, M.; Dong, J.; Kasagi, N.; Mori, T.; Ueda, H. Direct construction of an open-sandwich enzyme immunoassay for one-step noncompetitive detection of thyroid hormone T4. *Anal. Chem.* **2011**, *83*, 1008−1014.
(19) Ohmuro-Matsuyama, Y.; Inagaki, M.; Ueda, H. Detection of Protein Phosphorylation by Open-Sandwich Immunoassay. *Integrative Proteomics* **2012**, 197−214.
(20) Dong, J. H.; Shichiri, M.; Chung, C. I.; Shibata, T.; Uchida, K.; Hagihara, Y.; Yoshida, Y.; Ueda, H. An open sandwich immunoassay for detection of 13(R,S)-hydroxy-9(E),11(E)-octadecadienoic acid. *Analyst* **2017**, *142* (5), 787−793.
(21) Mohanty, N.; Berry, V. Graphene-Based Single-Bacterium Resolution Biodevice and DNA Transistor: Interfacing Graphene Derivatives with Nanoscale and Microscale Biocomponents. *Nano Lett.* **2008**, *8* (12), 4469−4476.
(22) Ohno, Y.; Maehashi, K.; Yamashiro, Y.; Matsumoto, K. Electrolyte-gated graphene field-effect transistors for detecting pH and protein adsorption. *Nano Lett.* **2009**, *9* (9), 3318−22.
(23) Ohno, Y.; Maehashi, K.; Matsumoto, K. Label-free biosensors based on aptamer-modified graphene field-effect transistors. *J. Am. Chem. Soc.* **2010**, *132* (51), 18012−3.
(24) Ohno, Y.; Maehashi, K.; Matsumoto, K. Chemical and biological sensing applications based on graphene field-effect transistors. *Biosens. Bioelectron.* **2010**, *26* (4), 1727−30.
(25) Ono, T.; Oe, T.; Kanai, Y.; Ikuta, T.; Ohno, Y.; Maehashi, K.; Inoue, K.; Watanabe, Y.; Nakakita, S.; Suzuki, Y.; Kawahara, T.; Matsumoto, K. Glycan-functionalized graphene-FETs toward selective detection of human-infectious avian influenza virus. *Jpn. J. Appl. Phys.* **2017**, *56*, 030302.
(26) Kawata, T.; Ono, Y.; Y, K.; Ohno, K.; Maehashi, K.; Inoue, K.; Matsumoto, K. Improved sensitivity of a graphene FET biosensor using porphyrin linkers. *Jpn. J. Appl. Phys.* **2018**, *57*, 065103.
(27) Ono, T.; Kanai, Y.; Inoue, K.; Watanabe, Y.; Nakakita, S. I.; Kawahara, T.; Suzuki, Y.; Matsumoto, K. Electrical Biosensing at Physiological Ionic Strength Using Graphene Field-Effect Transistor in Femtoliter Microdroplet. *Nano Lett.* **2019**, *19* (6), 4004−4009.
(28) Li, C.; Curreli, M.; Lin, H.; Lei, B.; Ishikawa, F. N.; Datar, R.; Cote, R. J.; Thompson, M. E.; Zhou, C. Complementary detection of prostate-specific antigen using In2O3 nanowires and carbon nanotubes. *J. Am. Chem. Soc.* **2005**, *127* (36), 12484−5.
(29) Kim, A.; Ah, C. S.; Yu, H. Y.; Yang, J. H.; Baek, I. B.; Ahn, C. G.; Park, C. W.; Jun, M. S.; Lee, S. Ultrasensitive, label-free, and real-time immunodetection using silicon field-effect transistors. *Appl. Phys. Lett.* **2007**, *91* (10), 103901.
(30) Ishikawa, F. N.; Chang, H. K.; Curreli, M.; Liao, H. I.; Olson, C. A.; Chen, P. C.; Zhang, R.; Roberts, R. W.; Sun, R.; Cote, R. J.; Thompson, M. E.; Zhou, C. W. Label-Free, Electrical Detection of the SARS Virus N-Protein with Nanowire Biosensors Utilizing Antibody Mimics as Capture Probes. *ACS Nano* **2009**, *3* (5), 1219−1224.
(31) Lee, C. S.; Kim, S. K.; Kim, M. Ion-Sensitive Field-Effect Transistor for Biological Sensing. *Sensors* **2009**, *9* (9), 7111−7131.
(32) Lee, N. K.; Sowa, H.; Hinoi, E.; Ferron, M.; Ahn, J. D.; Confavreux, C.; Dacquin, R.; Mee, P. J.; McKee, M. D.; Jung, D. Y.; Zhang, Z.; Kim, J. K.; Mauvais-Jarvis, F.; Ducy, P.; Karsenty, G. Endocrine regulation of energy metabolism by the skeleton. *Cell* **2007**, *130* (3), 456−69.
(33) Oury, F.; Khrimian, L.; Denny, C. A.; Gardin, A.; Chamouni, A.; Goeden, N.; Huang, Y. Y.; Lee, H.; Srinivas, P.; Gao, X. B.; Suyama, S.; Langer, T.; Mann, J. J.; Horvath, T. L.; Bonnin, A.; Karsenty, G. Maternal and offspring pools of osteocalcin influence brain development and functions. *Cell* **2013**, *155* (1), 228−41.
(34) Oury, F.; Sumara, G.; Sumara, O.; Ferron, M.; Chang, H.; Smith, C. E.; Hermo, L.; Suarez, S.; Roth, B. L.; Ducy, P.; Karsenty, G. Endocrine regulation of male fertility by the skeleton. *Cell* **2011**, *144* (5), 796−809.
(35) Sangawa, T.; Tabata, S.; Suzuki, K.; Saheki, Y.; Tanaka, K.; Takagi, J. A multipurpose fusion tag derived from an unstructured and hyperacidic region of the amyloid precursor protein. *Protein Sci.* **2013**, *22* (6), 840−850.
(36) Wongso, D.; Dong, J.; Ueda, H.; Kitaguchi, T. Flashbody: a next generation Fluobody with fluorescence intensity enhanced by antigen binding. *Anal. Chem.* **2017**, *89* (12), 6719−6725.
(37) Fan, Y.; Shi, S.; Ma, J.; Guo, Y. A paper-based electrochemical immunosensor with reduced graphene oxide/thionine/gold nanoparticles nanocomposites modification for the detection of cancer antigen 125. *Biosens. Bioelectron.* **2019**, *135*, 1−7.
(38) Mao, S.; Chang, J.; Pu, H.; Lu, G.; He, Q.; Zhang, H.; Chen, J. Two-dimensional nanomaterial-based field-effect transistors for chemical and biological sensing. *Chem. Soc. Rev.* **2017**, *46* (22), 6872−6904.
(39) Park, M.; Cella, L. N.; Chen, W.; Myung, N. V.; Mulchandani, A. Carbon nanotubes-based chemiresistive immunosensor for small molecules: detection of nitroaromatic explosives. *Biosens. Bioelectron.* **2010**, *26* (4), 1297−301.
(40) Long, F.; Zhu, A.; Shi, H.; Wang, H. Hapten-grafted graphene as a transducer for homogeneous competitive immunoassay of small molecules. *Anal. Chem.* **2014**, *86* (6), 2862−6.
(41) Chen, X.; Liu, Y.; Fang, X.; Li, Z.; Pu, H.; Chang, J.; Chen, J.; Mao, S. Ultratrace antibiotic sensing using aptamer/graphene-based field-effect transistors. *Biosens. Bioelectron.* **2019**, *126*, 664−671.

https://dx.doi.org/10.1021/acssensors.9b02137
ACS Sens. 2020, 5, 24−28